

Depletion interaction in a quasi-two-dimensional colloid assembly

Derek Frydel and Stuart A. Rice

Department of Chemistry and The James Franck Institute, The University of Chicago, Chicago, Illinois 60637, USA

(Received 1 October 2004; revised manuscript received 7 January 2005; published 12 April 2005)

We address several aspects of the character of the depletion interaction in a quasi-two-dimensional (Q2D) colloid system. First, we consider how, given information concerning the pair and triplet correlation functions, the depletion interaction can be efficiently and accurately determined. For this purpose we introduce a method based on the Born-Green equation using the assumption that for the Q2D binary mixtures of interest to us the depletion interaction is accurately represented as a sum of pair potentials. We then verify, by direct calculation, that three-particle contributions to the depletion interaction are negligibly small in the region of thermodynamic state space of interest to us. Second, we develop a representation of the dependence of the depletion interaction in a Q2D colloid system on the thickness of the confining parallel plates. Third, we report the results of extensive simulations of Q2D binary hard-sphere mixtures for a range of cell thickness, large and small particle number densities, and a ratio of sphere diameters $q=0.3$.

DOI: 10.1103/PhysRevE.71.041402

PACS number(s): 82.70.Dd, 61.20.Ja, 61.20.Lc, 66.30.-h

I. INTRODUCTION

It has been known for many years that the pair correlation function of a dense one-component hard-sphere fluid exhibits a pronounced peak at a center-to-center separation of one sphere diameter, thereby implying that the potential of mean force is attractive at that distance. The origin of this attractive potential of mean force between particles that have no attractive component in their direct interaction potential has also been understood for many years; it arises from the exclusion of third-body hard spheres from the region between two hard spheres when the separation of the centers of the latter is less than two sphere diameters. The potential of mean force is, in this case, entirely of entropic origin, and it is density dependent.

The existence of an attractive interaction between, say, large hard-sphere colloid particles in a binary mixture with small hard-sphere colloid particles, commonly called the depletion interaction, can be traced to the same origin [1]. In a binary mixture the full depletion potential is a many-body interaction with a dominant two-body term. Indeed, representing the depletion interaction as a sum of pair potentials has been found to give predictions that are in excellent agreement with the results of simulations of hard-sphere binary mixtures [2]. Specifically, each n -body term of the multibody expansion of the depletion interaction embodies both direct and indirect contributions. The three-body term is found to be significantly weaker than the two-body term even with the direct contribution present, and its range is similar to that of the two-body term [3–5]. A direct three-body contribution to the depletion potential arises when the diameter of the small particle is too large to fit into the cavity formed when three large particles are in contact, which occurs when the diameter ratio is $q < 2/\sqrt{3} - 1 = 0.1547$.

To date, almost all theoretical studies of the depletion interaction have dealt with three-dimensional systems. However, there is also considerable interest in systems in confined spaces with various geometries. Castañeda-Priego, Rodríguez-López, and Méndez-Alcaraz [6] have studied the

depletion interaction in a strictly two-dimensional binary mixture of hard disks. We note that the difference between quasi-two-dimensional (Q2D) and 2D confinement can play a role in determining system properties. Depending on the size ratio of the species in a binary mixture and the ratio of wall spacing to small-particle diameter, one can easily generate systems in which the large particles move in a Q2D domain, but the small particles, which are the source of depletion interaction, move in three dimensions. In this paper we study the depletion interaction and how it changes continuously as the system geometry changes from the 3D to confined Q2D geometry. We accomplish this by changing the confining plate separation from a value equal to the large-particle diameter to a value where the depletion interaction no longer changes with an increasing separation.

The influence of a wall on the depletion interaction can conveniently be thought of as generated by the three-body interaction between two large spheres and a wall (or another sphere with an infinitely large radius). This analogy allows us to make a number of assertions, based on what is already known about the three-body contribution to the depletion interaction, concerning the influence of a wall on the two-body depletion interaction between large spheres. First, the wall contribution to the interaction should be much weaker than the depletion interaction between two large spheres. Second, the direct wall-particle contribution to the interaction should come into play when the diameter ratio $q > 0.25$. Finally, the range of the wall contribution to the depletion interaction should be no larger than that for the depletion interaction between two large spheres. As the four-body contribution to the depletion interaction is even less significant than the three-body contribution, we postulate that the presence of the second wall in the Q2D geometry will generate no extra four-body effect.

Here a comment is in order. The three-body contribution to liquid properties is dependent on density. This density dependence arises because the chance that three particles collide simultaneously increases with increasing density. On the other hand, the wall contribution (thought of as the third-body contribution) is independent of colloid density but in-

stead depends on the wall separation. When the wall separation is small enough, the wall contribution is a constant factor. In this respect the wall contribution to the depletion interaction can be expected to be more significant than the three-body contribution.

This paper addresses several aspects of the character of the depletion interaction in a Q2D colloid system. First we consider how, given information concerning the pair and triplet correlation functions, the depletion interaction can be efficiently and accurately determined. For this purpose we introduce a method based on the Born-Green (BG) equation using the assumption that for the Q2D binary mixtures of interest to us the depletion interaction is accurately represented as a sum of pair potentials. We then verify, by direct calculation, that three-particle contributions to the depletion interaction are negligibly small in the region of thermodynamic state space of interest to us. Second, we develop a representation of the dependence of the depletion interaction in a Q2D colloid system on the separation of the confining parallel plates. Third, we report the results of extensive simulations of Q2D binary hard-sphere mixtures for a range of cell thickness, large- and small-particle number densities, and the ratio of sphere diameters $q=0.3$.

II. EXTRACTING THE DEPLETION POTENTIAL FROM THE PAIR AND TRIPLET CORRELATION FUNCTIONS: BORN-GREEN EQUATION APPROACH

We start our analysis with a few generalizations concerning the character of the depletion interaction. We restrict our attention to the case of a binary mixture, but formal generalization to the case of multicomponent mixtures is straightforward. As first shown by McMillan and Mayer [7], it is possible to describe a binary mixture of, say, α and β species, as if it were an effective one-component α -species system with the direct $\alpha\alpha$, $\beta\beta$, and $\alpha\beta$ interactions replaced by an $\alpha\alpha$ free energy of interaction; the latter is obtained by integrating over the positions of all the particles of species β . After the degrees of freedom of β are integrated out, the resulting effective one-component fluid can be described by an effective Hamiltonian containing a volume term, to which only the β particles contribute, a one-body term in which a single α particle in a fluid of β particles contributes, a two-body term, a three-body term, and so on. In the three-dimensional case, for mixtures in which the ratio of particle diameters, q , is small, the most important contributions are found to come from the one-body and two-body terms in the effective Hamiltonian. The three-body and higher-order terms never vanish under all conditions, but are found to make negligible contributions to the effective interaction for a wide range of conditions. Specifically, if two particles of species α are separated by a distance \mathbf{r} and are embedded in a fluid of species β with chemical potential μ_β , the effective potential acting between the α particles has the form [8,9]

$$V_{eff} = u_{\alpha\alpha}(\mathbf{r}) - k_B T [c_\alpha^{(1)}(\mathbf{r}, \mu_\alpha, \mu_\beta, T) - c_\alpha^{(1)}(\infty, \mu_\alpha, \mu_\beta, T)], \quad (1)$$

in which $u_{\alpha\alpha}$ is the direct interaction potential between two particles of species α and $c_\alpha^{(1)}$ is the one-body direct correla-

tion function of species α . It has been shown that the depletion potential between two large hard spheres (and between a hard sphere and a smooth wall) has both attractive and repulsive parts as well as oscillatory behavior that can be traced to correlation effects associated with the small hard spheres.

We now develop a convenient and accurate method for calculating the depletion interaction in a binary hard-sphere colloid mixture from knowledge of the pair and triplet correlation functions obtained from simulations or from video microscopy. We are interested in determining if the Yvon-Born-Green (YBG) integro-differential equation can be used to calculate the depletion potential accurately. This equation relates the pair and triplet correlation functions $g_2(r)$ and $g_3(\mathbf{r}_1, \mathbf{r}_2, \mathbf{r}_3)$, respectively, to the pair potential $u_2(r)$ when more than two-body interactions are absent. The YBG equation for a homogeneous liquid is

$$\nabla_{\mathbf{r}_1} [w_2(r_{12}) - u_2(r_{12})] = \frac{\rho}{g_2(r_{12})} \int_V d\mathbf{r}_3 \nabla_{\mathbf{r}_1} u_2(r_{13}) g_3(\mathbf{r}_1, \mathbf{r}_2, \mathbf{r}_3), \quad (2)$$

in which r_{ij} is the distance between particles i and j , \mathbf{r}_i is the position of particle i , and $w_2(r)$ is the potential of the mean force defined by

$$g_2(r) = \exp[-\beta w_2(r)]. \quad (3)$$

Equation (2) can be simplified to read

$$\frac{\partial}{\partial r} [w_2(r) - u_2(r)] = \frac{\rho}{g_2(r)} \int_0^\infty ds s \frac{\partial u_2(s)}{\partial s} f(r, s). \quad (4)$$

Here $r = |\mathbf{r}_1 - \mathbf{r}_2|$, $s = |\mathbf{r}_1 - \mathbf{r}_3|$, and the function $f(r, s)$ depends on the system. For a two-dimensional liquid we have

$$f(r, s) = 2 \int_0^\pi d\theta_{rs} \cos(\theta_{rs}) g_3(r, s, \theta_{rs}), \quad (5)$$

where θ_{rs} is the angle between the vectors \mathbf{r} and \mathbf{s} . We now suppose that the depletion interaction u_d is the effective pair interaction in the fluid and we make the replacement $u_2 = u_d$. Here u_d is generally dependent on the density of small particles and temperature ($u_d \equiv u_d[\beta, \eta_s]$), where for hard spheres the temperature dependence is linear. Equation (4) can be further modified by observing that for the hard-core interaction $\beta \partial u_d(r) / \partial r|_{r=\sigma} = -\delta(r - \sigma)$, so that

$$\frac{\partial u_d(r)}{\partial r} = \frac{\partial w_2(r)}{\partial r} + \frac{\beta^{-1} \rho}{g_2(r)} \left(\sigma f(r, \sigma) - \int_\sigma^\infty ds s \frac{\partial u_d(s)}{\partial s} f(r, s) \right). \quad (6)$$

The function $f(r, s)$ needed to solve Eq. (6) will be obtained from simulation of binary systems. Specifically $f(r, s)$ will be calculated for the set of grid points $\{r_m, s_n\}$:

$$f(r_m, s_n) = \frac{1}{4\pi r_m s_n N p^2} \times \left\langle \sum_{i \neq j \neq k}^N \delta^\Delta(r_m - r_{ij}) \delta^\Delta(s_n - r_{ik}) \cos \theta_{r_{ij} s_{ik}} \right\rangle. \quad (7)$$

In Eq. (7), $r_m = \Delta(m+0.5)$ and $s_n = \Delta(n+0.5)$ where m and n are integers and Δ is the bin size. The function $\delta^\Delta(x-a)$ is defined as

$$\delta^\Delta(x-a) = \begin{cases} 0, & a - \Delta/2 > x \geq a + \Delta/2, \\ 1/\Delta, & a - \Delta/2 \leq x < a + \Delta/2. \end{cases}$$

The resulting function $f(r_m, s_n)$ is stored in a two-dimensional array f_{mn} . The bin size Δ was set to 0.01σ . The calculation of f_{mn} requires the identification of all triplet configurations for a single-particle configuration. This is a time-consuming step since for each configuration a triple loop is executed. However, we expect u_d to be short ranged. Accordingly, we chose a cutoff distance of 2σ so all the triplets that contribute to f_{mn} where $r, s > 2\sigma$ need not be identified. This procedure reduces the computer time needed to a time that is comparable to that used when calculating a pair correlation function.

In order to test how well the doublet and triplet distribution functions can reproduce the pair potential based on the relation in Eq. (2), we carried out simulations for systems with one type of particle interacting via a known pair interaction. The pair interaction we chose for this test is

$$\beta u_d(r) = -\frac{1+q}{2q} [(\eta_s^r) 3x^2 + (\eta_s^r)^2 (9x + 12x^2) + (\eta_s^r)^3 (36x + 30x^2)] \quad \text{for } -1 < x < 0, \quad (8)$$

where $x = (r/\sigma - 1 - q)/q$. This is the expression for the depletion potential in 3D for hard spheres in a binary mixture up to third order in η_s^r within the Derjaguin framework [10]. However, any other pair interaction would be as good for test purposes.

Two pair interactions, corresponding to the parameters $(q=0.3, \eta_s^r=0.1)$ and $(q=0.6, \eta_s^r=0.13)$ were used. Once $g_2(r)$ and $f(r, s)$ were obtained from the simulation, we solved Eq. (4) iteratively taking $w_2(r)$ as an initial estimate for $u_d(r)$. The calculated form for $u_d(r)$, together with $u_d(r)$ from Eq. (8) and the discrepancy between the two, are shown in Fig. 1. Our procedure is seen to give very good results. The spike in the error plot results from a nonsmooth singular point in $u_d(r)$ at $r=q$.

The method of calculating the pair interaction based on the Born-Green equation that we have suggested offers an alternative route to the inversion methods generally used for this purpose [11,12]. In definition our depletion potential is equivalent to the depletion potential calculated by the authors of Ref. [6] who also define the depletion potential as an effective pair potential due to the second-particle component. These authors used the integral equation theory method.

The method just described for the calculation of u_d makes no provision for the possibility that a three-body interaction

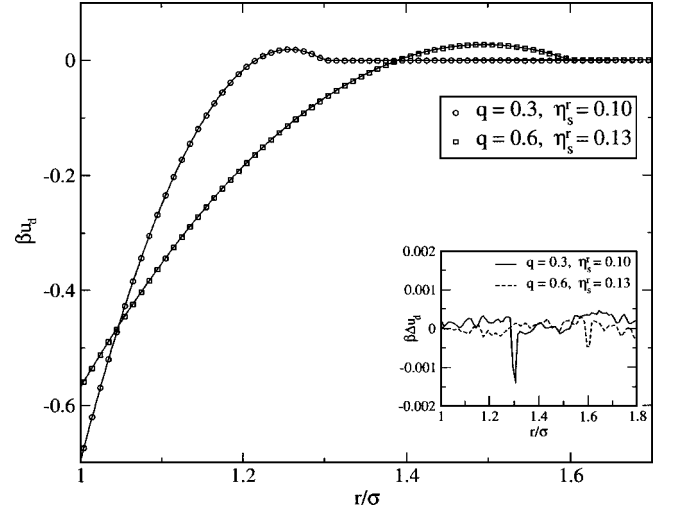


FIG. 1. Pair potentials as calculated from the YBG relation described in Sec. II and compared with the exact pair potentials in Eq. (8). The calculations were done at density $\rho\sigma^2=0.85$.

acts in the system of interest. The complete depletion interaction is a many-body free energy with a dominant two-body term. However, the three-body contribution to the depletion interaction is not negligible for all values of q or everywhere in the thermodynamic state space. If the three-body contribution is not negligible, it can influence the pair potential calculated from the BG equation, so that the calculated pair potential will incorporate some averaged contribution from three-body interactions.

The BG equation is not valid when the three-body contribution to the particle interaction is nonzero. By differentiating $g_2(r)$ with respect to particle separation and assuming three-body interactions to be present, we get the following expression:

$$\begin{aligned} \nabla_{\mathbf{r}_1}[\phi(r_{12}) - u_2(r_{12})] &= \frac{\rho}{g_2(r_{12})} \int_V d\mathbf{r}_3 \nabla_{\mathbf{r}_1} u_2(r_{13}) g_3(\mathbf{r}_1, \mathbf{r}_2, \mathbf{r}_3) \\ &+ \frac{\rho}{g_2(r_{12})} \int_V d\mathbf{r}_3 \nabla_{\mathbf{r}_1} u_3(r_{12}, r_{13}, r_{23}) \\ &\times g_3(\mathbf{r}_1, \mathbf{r}_2, \mathbf{r}_3) + \frac{\rho}{2g_2(r_{12})} \\ &\times \int_V d\mathbf{r}_3 \int_V d\mathbf{r}_4 \nabla_{\mathbf{r}_1} u_3(r_{12}, r_{13}, r_{23}) \\ &\times g_4(\mathbf{r}_1, \mathbf{r}_2, \mathbf{r}_3, \mathbf{r}_4). \end{aligned} \quad (9)$$

When cast in the form of Eq. (4) an additional function $R(r)$ appears:

$$\frac{\partial}{\partial r}[\phi(r) - u_2(r)] = \frac{\rho}{g_2(r)} \int_0^\infty ds s \frac{\partial u_2(s)}{\partial s} f(r, s) + R(r), \quad (10)$$

where $R(r)$ incorporates the contribution from the three-body potential. In order to get the exact two-body part of the

depletion potential when there are three-body interactions we must know $R(r)$. This however is, in general, impossible. When, instead, we neglect the term $R(r)$ and use Eq. (4), the potential that we arrive at is an effective interaction. Strictly speaking, this effective interaction cannot reproduce any property of the actual system exactly; nor is it designed to yield any one particular property of the physical system exactly. By use of suitable constraints, the effective pair interaction can be modeled to yield any one, but not all, of the fluid pressure, energy, or pair distribution function [13–16] correctly. The accuracy of our results depends on the strength of the three-body interaction; if the three-body contributions to the fluid properties are insignificant, our effective potential should be in very good agreement with the true two-body part of the depletion potential. The best test of this influence is to compare the results of simulation of the one-component system interacting via the effective pair depletion potential with the results for the binary system. We show below that this comparison yields excellent agreement, implying that the three-body contribution to the depletion interaction is negligible even for diameter ratios $q > 0.1547$.

III. SIMULATIONS

We have carried out two sets of simulations of Q2D binary hard-sphere mixtures. The first set of simulations used the (N, z_s, A, H) ensemble. N is the number of large particles, z_s is the fugacity of the small particles, and A is the area and H the height of the containing cell. This ensemble represents large particles in a space of height H between two hard walls immersed in a reservoir of small particles with density ρ_s^r . For hard spheres there is no dependence of the thermodynamic properties on temperature. The number of large particles is fixed at $N=400$ and the hard plates are at $z=H/2$ and $z=-H/2$; hence, the sphere centers are restricted to $-(H-\sigma)/2 < z < (H-\sigma)/2$. The simulation algorithm directly controls z_s , but in order to be able to control ρ_s^r , we use the relation $\rho_s^r \exp(\beta\mu_s^{ex}) = z_s$, where μ_s^{ex} is the excess chemical potential of the small spheres. We have used the Carnahan-Starling equation of state to calculate μ_s^{ex} , since that equation of state is very accurate in the density regime of interest.

The Born-Green relation which was used to obtain the depletion interaction is for a homogeneous 2D liquid. The Q2D system allows out-of-plane motion of the large particles, which may obscure our results with contributions from slightly out-of-plane positions of large particles in the z direction. To avoid this problem we constrain the large-particle centers to a strictly two-dimensional plane regardless of the plate separation. No constraints are imposed on the small-sphere motion. This procedure allows us to calculate the depletion potential between large spheres at fixed distance from the walls rather than for particles at different distances from the walls. Given that the three- and higher-body terms of the depletion potential are negligible, our scenario is equivalent to that of calculating the depletion interaction between two large spheres immersed in the sea of small spheres at fixed distance from the walls.

The density of the large particles is defined as $\rho = N/A$ and the packing fraction of the small particles as η_s

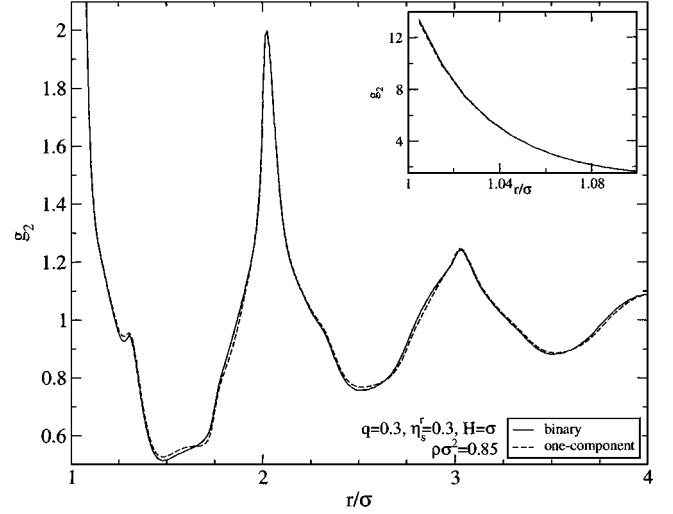


FIG. 2. The pair correlation functions of a binary hard-sphere mixture and the corresponding effective one-component system for the plate separation $H=\sigma$, density $\rho\sigma^2=0.85$, and $\eta_s^r=0.3$. The inset contains a close-up of the pair correlation functions near the contact value.

$= \pi\sigma_s^3 N_s / (6HA)$, where N_s and σ_s denote the number and diameter of small particles, respectively.

IV. RESULTS OF SIMULATIONS

All of the simulations in the (N, z_s, A, H) ensemble were carried out with the density of large particles $\rho\sigma^2=0.85$ and the diameter ratio $q=0.3$. The high liquid density was chosen to facilitate calculations since at high density fewer small particles are required for a given z_s . The size ratio $q=0.3$ was selected to include the direct contribution to the three-body depletion interaction as well as to facilitate calculations. It is within the range commonly used in the experimental studies. To ensure that the collected configurations are not limited to a local minimum, a potential ergodicity problem when simulating asymmetric binary mixtures, each system was equilibrated from two different initial configurations, both perfect triangular lattice crystals, one distributed throughout the whole cell with the lattice constant $\Delta = \sqrt{2/(\rho\sqrt{3})}$ where $\rho\sigma^2=0.85$ and the other confined to one part of the cell with the lattice constant $\Delta \leq \sqrt{2/(\rho_m\sqrt{3})}$ where $\rho_m\sigma^2 \approx 0.91$ is approximately the melting density of a hard disk and Q2D hard-sphere solid [17]. For all cases covered in this work we find that the two initial conditions evolve to the same final state. Furthermore, a number of calculations performed at lower density (see later) produce the same depletion interaction, providing further assurance that the system is not frozen in a metastable region.

A. Three- and higher-body terms of the depletion interaction

In this section we examine the three- and higher-body contributions to the depletion interaction. We first compare the pair correlation functions of a binary hard-sphere mixture and the corresponding effective one-component system (Fig.

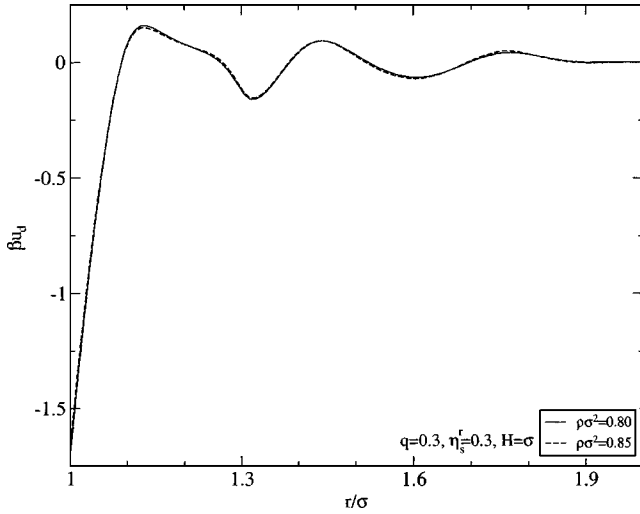


FIG. 3. The density dependence of the effective depletion pair potentials for the plate separation $H=\sigma$ and $\eta_s^f=0.3$. For a strictly two-body depletion interaction, there should be no density dependence in the effective depletion pair interaction.

2) for $\eta_s^f=0.3$ at $H=\sigma$ and density $\rho\sigma^2=0.85$. The two pair correlation functions compare very well. The biggest mismatch occurs at contact separation $r=\sigma$ where g_2 of the effective one-component system slightly underestimates g_2 for the binary system.

Next, we investigate the density dependence of the depletion pair potential, $u_d(r)$, calculated from the Born-Green relation [Eq. (6)]. As the density increases, the three-body contribution becomes more important because there is a greater probability for particle triplets to come within the range of the three-body interaction. Figure 3 shows $u_d(r)$ for $\eta_s^f=0.3$ at plate height $H=\sigma$ for densities $\rho\sigma^2=0.8$ and $\rho\sigma^2=0.85$. Even for this high density of small particles, we find only a very small change due to the density increase, indicating that the three- and higher-body contributions to the depletion interaction are very small and do not affect our results.

As follows from a uniqueness theorem for the pair correlation function [18], a pair potential can be designed to reproduce the pair correlation function of the system with three- and higher-body terms, but it cannot be designed to reproduce the triplet and higher-order correlation functions. This fact can easily be demonstrated if we consider the low-density limit for a system with only two-body interactions, $\lim_{\rho \rightarrow 0} g_3(r, s, t) = \exp\{-\beta[u_2(r) + u_2(s) + u_2(t)]\}$, and for a system with three-body interactions, $\lim_{\rho \rightarrow 0} g_3(r, s, t) = \exp\{-\beta[u_2(r) + u_2(s) + u_2(t)]\} \exp[-\beta u_3(r, s, t)]$. In this simplified limit it can be seen that no two-body term can substitute in an exact manner for the explicit three-body contribution in g_3 . Though our effective pair potential was not designed to specifically reproduce a pair distribution function exactly, nonetheless it does well in this respect (Fig. 2). Consequently, the discrepancy between the g_3 's of the two-component and the effective one-component system is a good measure of the three-body contribution to the particle interactions.

To compare the structure of a binary system and an effective single-component system, we measure the triplet distribution

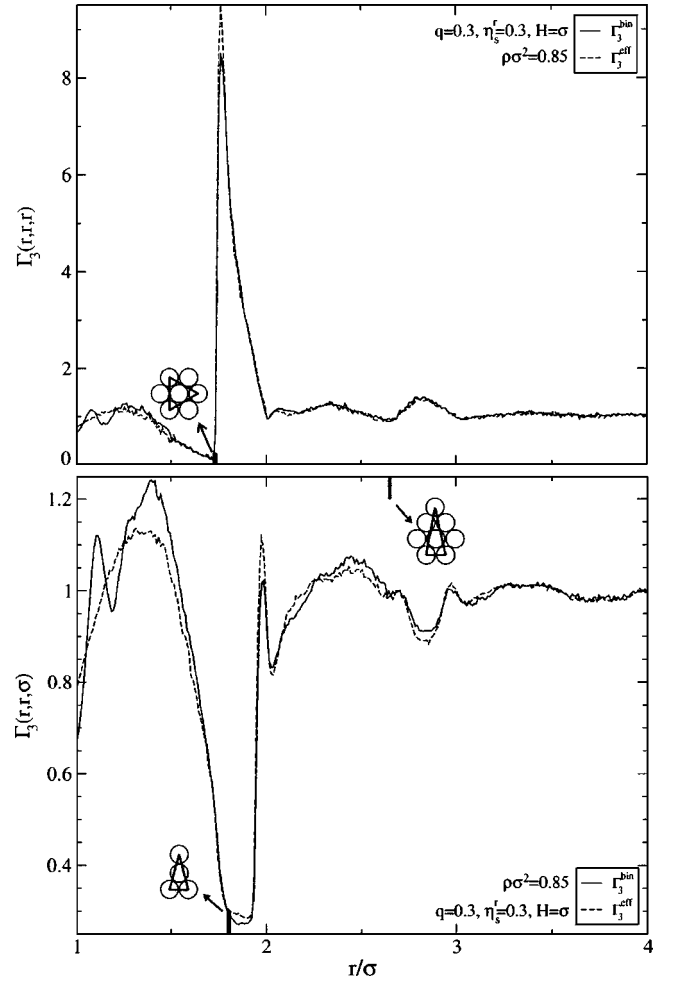


FIG. 4. Γ_3 [Eq. (11)] for the two- and the effective one-component systems for the density $\rho\sigma^2=0.85$, the plate separation $H=\sigma$, and $\eta_s^f=0.3$.

bution functions for equilateral (r, r, r) and isosceles (r, r, σ) triplet configurations normalized to the Kirkwood superposition product of pair correlation functions:

$$\Gamma_3(r, s, t) = \frac{g_3(r, s, t)}{g_2(r)g_2(s)g_2(t)}. \quad (11)$$

For $\eta_s^f=0.19$ and $\eta_s^f=0.25$ the agreement between Γ_3 for the effective one-component and binary system is very good. For $\eta_s^f=0.3$ the difference between the two is more significant especially at small r . Figure 4 shows Γ_3 for the two- and effective one-component systems for density $\rho\sigma^2=0.85$ and plate separation $H=\sigma$, for different values of the small-particle packing fraction. The function Γ_3 for the binary system displays modulations which are absent in the pair representation of the binary system.

It is useful to make a few comments regarding the performance of the Kirkwood superposition approximation. This approximation fails on account of the formation of local order. As the density increases, the liquid develops a local angular order which anticipates the solid structure. For $\Gamma_3(r, r, r)$ the superposition approximation underestimates the presence of equilateral triangles big enough to enclose a

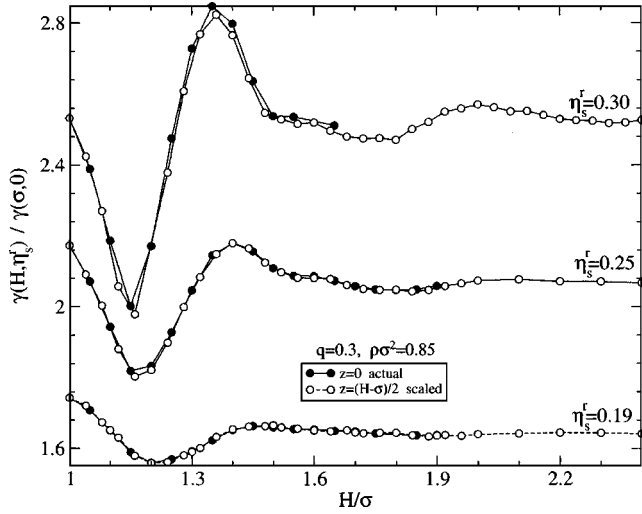


FIG. 5. The pair correlation contact values $\gamma(H, \eta_s^r)$ as a function of the plate separation H . Here $\gamma(H, \eta_s^r)$ for the case where the large spheres are at the wall contact is scaled according to the formula $2\gamma(2H-\sigma, \eta_s^r) - \gamma(\sigma, \eta_s^r)$.

single particle. On the other hand, the presence of equilateral triangles too small to enclose a particle is overestimated by the superposition approximation. For $\Gamma_3(r, r, \sigma)$ the superposition approximation overestimates the presence of isosceles triangles large enough to host a particle internally, a configuration that is unfavorable for the local triangular symmetry. The superposition approximation performs slightly worse for the pure hard-sphere system than for the binary mixtures that we have studied, since the latter are more disordered at $\rho\sigma^2=0.85$.

B. Influence of the walls on the depletion interaction

To be able to gauge the manner and extent of the influence that the slit geometry walls produce on the depletion interaction between large spheres at given η_s^r , we show in Fig. 5 how the contact value of the pair distribution function between large spheres, $g_2(\sigma)$, whose centers are constrained to the 2D plane, changes with the plate separation for different η_s^r . We use the symbol $\gamma(H, \eta_s^r)$ to denote $g_2(\sigma)$ at given H and η_s^r . For the system with large particles in wall contact we scale $\gamma(H, \eta_s^r)$ according to the formula $2\gamma(2H-\sigma, \eta_s^r) - \gamma(\sigma, \eta_s^r)$. If the influence of both cell walls on the depletion interaction is a sum of the individual wall contributions, the two plots should overlap. It can be seen in Fig. 5 that the resulting data points indeed overlap (the visible discrepancies lie within the statistical error); thus, the contribution of two walls is an additive effect and the presence of the second wall does not produce a four-body effect between two spheres and two walls.

The range of the wall influence on the depletion interaction is of order a small particle diameter; for $H > 1.6\sigma$, a small particle can fit between a large particle and a wall and $\gamma(H, \eta_s^r)$ begins approaching the homogeneous liquid limit. The wall influence on the depletion interaction does not affect a monotonic trend with increasing plate separation, but

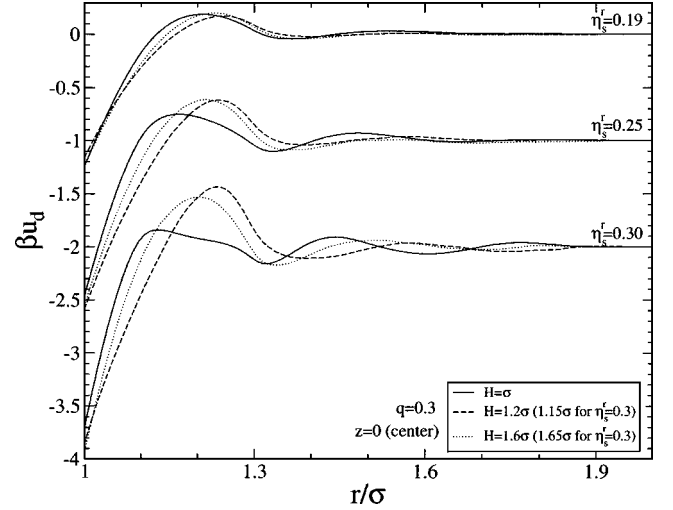


FIG. 6. Depletion potentials for different plate separations and packing fractions of small particles. The potentials have been shifted for better presentation.

instead has a modulating character; it can reduce or enhance the depletion interaction, depending on the distance of large particles from a wall.

Figure 6 shows the depletion interaction calculated from the Born-Green relation [Eq. (6)] as an effective pair potential. For each η_s^r we plot the depletion potentials for plate separations that are of most interest: $H=\sigma$, H corresponding to the minimum of the plot in Fig. 5, and large H where the depletion interaction is close to the homogeneous 3D limit. The depletion potential most strongly influenced by the presence of the wall is that for $H=\sigma$. Its repulsive barrier and range are reduced. As the plate separation increases to $H \approx 1.2\sigma$, the barrier and range of the depletion potential increases. At large plate separation both the range and barrier are slightly reduced and the depletion potential stops changing with the changing plate separation as the 3D homogeneous limit is approached. For $\eta_s^r=0.19$ the influence of the wall on the depletion interaction is very small as little change is produced by increasing H . At $\eta_s^r=0.30$, on the other hand, the repulsive barrier at $H=\sigma$ almost completely disappears.

In Fig. 7 we plot the difference between the two-body depletion potentials for $H=\sigma$ and large H corresponding to the 3D homogeneous limit, $\Delta u_3(r) = u_d(r; H=\sigma) - u_d(r; H=\text{large})$. This will allow us to extract a pure wall contribution to the pair depletion potential when $H=\sigma$. The resulting wall contribution is very similar, qualitatively and quantitatively, to the three-body contribution to the depletion interaction calculated in Ref. [5]; as in Ref. [5], $\Delta u_3(r)$ is highly modulated, reflecting correlations between the small particles. It is much smaller than the two-body depletion potential, and its range is similar to that of the pair depletion interaction.

The results presented above suggest that the wall contribution to the depletion interaction is visible but not very strong. For a low density of small particles ($\eta_s^r=0.19$) the depletion potential hardly changes with distance to the wall. The depletion interaction, as may be expected, is most strongly affected by the wall contribution at the limit of confinement (when the plate separation equals a large particle

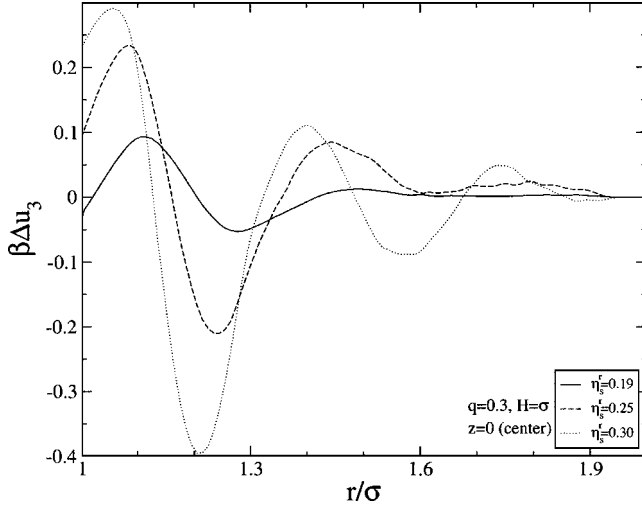


FIG. 7. The difference between the effective pair potentials at $H=\sigma$ and at large H , $\Delta u_3(r)=u_d(r;H=\sigma)-u_d(r;H=\text{large})$, for the system of the large spheres constrained to the xy plane at the center.

diameter). At this plate separation the range and repulsive barrier of the depletion interaction are reduced. Another conclusion of our study is that the wall contribution is not a monotonic function of distance to the wall, but instead is a modulating function of H . This is in agreement with our conjecture which claims that the wall contribution is in essence similar to a three-body contribution to the depletion interaction [5]. If the large particles were released from the requirement of lying in a plane and allowed to have an out-of-plane motion as is the case in experimental studies, the wall contribution would be even less significant since particles would occupy different positions relative to the walls.

V. VIRIAL EXPANSION FOR THE DEPLETION POTENTIAL IN CONFINED GEOMETRY

In this section we derive an expression for the depletion force between two large spheres immersed in the nonuniformly distributed sea of small particles. In our study the distortion of the small-particle density is affected by the walls of the cell. We use the local density approximation where density of small particles at each volume element is treated locally, ignoring the influence of density variations of a neighboring region. This model, by considering the small-particle density variation “literally,” represents a limiting case where effect of the walls on the depletion interaction is maximal. The comparison between the model and simulation results will allow us to gauge the extent of the nonlocal effects present in the real system. The density distribution of the small particles along the z axis used in our expression for the depletion force is calculated from the simulation at given H , η_s^c , and q where no large particles are present.

To carry out this investigation we use a virial expansion. We carry the expansion up to and including the third virial coefficient, as calculated by Mao *et al.* [19] for hard plates immersed in a hard-sphere liquid bath. We then use the Derjaguin approximation to apply those results to hard spheres.

In the following we provide a detailed description of the calculations. Two parallel hard plates placed inside a hard-sphere liquid (we assume the spheres are small for the sake of clarity) feel an outside and an inside pressure. The outside pressure is that for a homogeneous hard-sphere liquid,

$$\beta P_{out} = \rho_s^r + B_2 \rho_s^r{}^2 + B_3 \rho_s^r{}^3 + \dots, \quad (12)$$

where B_n are the usual virial coefficients [20]. The inside pressure, unlike the pressure outside, depends on the plate separation. When written in the form of a virial expansion we have

$$\beta P_{in}(h) = \rho_s^r + \mathcal{B}_2(h) \rho_s^r{}^2 + \mathcal{B}_3(h) \rho_s^r{}^3 + \dots \quad (13)$$

We reserve the small letter h for the plate separation, instead of the capital letter H , because as we transform Eqs. (12) and (13) to describe the depletion interaction between two large spheres, h will refer to the shortest distance between two large sphere surfaces and not the wall separation. The $\mathcal{B}_n(h)$ denote the h -dependent virial coefficients. For $h \leq \sigma_s$, $P_{in} = 0$ since no particle can enter the slit cell. In the limit $h \rightarrow \infty$, $\mathcal{B}_n(h) = B_n$, and $P_{in} = P_{out}$. For $h \leq \sigma_s$ the salvation “force” f_s , defined as the net pressure felt by a wall, is

$$\beta f_s = -P_{out} = -\rho_s^r - B_2 \rho_s^r{}^2 - B_3 \rho_s^r{}^3 - \dots \quad (14)$$

and, for $h > \sigma_s$,

$$\begin{aligned} \beta f_s(h) &= P_{in}(h) - P_{out} \\ &= \{\mathcal{B}_2(h) - B_2\} \rho_s^r{}^2 + \{\mathcal{B}_3(h) - B_3\} \rho_s^r{}^3 + \dots \end{aligned} \quad (15)$$

The depletion force between two plates with separation h expressed in terms of the solvation force is $f_d(h) = A f_s(h)$ where A is the area of a plate.

To calculate the depletion force between two large hard spheres (instead of the large hard plates) in the heterogeneously distributed small-particle liquid, we use two approximations. First, we use the Derjaguin approximation to deal with the sphere curvature [21]. Second, to deal with the heterogeneous small-particle distribution we use a local approximation where we assume that for an infinitesimal surface element the small-particle distribution is locally homogeneous and all the contributions are additive. The results are, for $h > \sigma_s$, where here h is the smallest distance between the surfaces of two large spheres,

$$\begin{aligned} f_d(h) &= 2\pi d^2 \int_0^{\pi/2} d\theta \sin \theta \cos \theta \{b_2(\theta, h) [\bar{\rho}_s^r(\theta)]^2 \\ &\quad + b_3(\theta, h) [\bar{\rho}_s^r(\theta)]^3 + \dots\} \end{aligned} \quad (16)$$

and, for $h \leq \sigma_s$,

$$\begin{aligned} f_d(h) &= 2\pi d^2 \int_{\theta_f(h)}^{\pi/2} d\theta \sin \theta \cos \theta \{b_2(\theta, h) [\bar{\rho}_s^r(\theta)]^2 \\ &\quad + b_3(\theta, h) [\bar{\rho}_s^r(\theta)]^3 + \dots\} \\ &\quad - 2\pi d^2 \int_0^{\theta_f(h)} d\theta \sin \theta \cos \theta \{B_2 [\bar{\rho}_s^r(\theta)]^2 \\ &\quad + B_3 [\bar{\rho}_s^r(\theta)]^3 + \dots\}. \end{aligned} \quad (17)$$

In Eqs. (16) and (17), $b_n(\theta, h) = \{\mathcal{B}_n(h + \sigma - 2d \cos \theta) - B_n\}$, $\theta_f(h) = \arccos[(h + \sigma)/2d]$, and $\bar{\rho}_s^r(\theta)$ is defined as

$$\bar{\rho}_s^r(\theta) = \frac{2}{\pi} \int_0^{\pi/2} d\phi \rho_s^r(d \sin \theta \cos \phi). \quad (18)$$

θ and ϕ are the angular degrees of freedom of the spherical coordinates where ϕ is the azimuthal angle. The origin coincides with the center of one of the particles. θ is measured from the direction $(\mathbf{R}_1 - \mathbf{R}_2)$ where \mathbf{R}_1 and \mathbf{R}_2 are the locations of the centers of the two large particles.

If we terminate the virial expansion at first order, we get an equivalent of the Asakura-Oosawa approximation. In rectangular coordinates this approximation reduces to

$$f_{AO}(h) = -4 \int_0^{z_f(h)} dz \rho_s^r(z) \sqrt{z_f^2(h) - z^2}, \quad (19)$$

where $z_f(h) = \sqrt{d^2 - (\sigma + h)^2/4}$ denotes the point on the z axis where two spherical shells of radius d separated by a distance $\sigma + h$ and located at the center of the cell cross. When the density of small spheres is made independent of z we get $\rho_s^r(z) = \rho_s^r$ and Eq. (19) retrieves the Asakura-Oosawa depletion force for a homogeneous liquid [22,10],

$$f_{AO}(h) = -4\rho_s^r \int_0^{z_f(h)} dz \sqrt{z_f^2(h) - z^2} = -\pi \rho_s^r z_f^2(h). \quad (20)$$

We have a few comments concerning the nature of the Derjaguin approximation. The Derjaguin approximation becomes exact in the limit $q \rightarrow 0$. As q increases, its performance is expected to worsen. However, it turns out that an additional source of error from truncating a virial expansion at third order cancels out the shortcomings of the Derjaguin approximation [10]. Thus the apparent success of the Derjaguin approximation within the third-order theory reported in Ref. [19] does not testify to good performance of this approximation, but is rather accidental, and inclusion of the fourth- and higher-order terms produces poorer results. The model described above was found to produce very good results for the uniform density of small particles in agreement with results reported in Ref. [19]. For the case of nonuniform density distribution of small particles, deviation from the simulation results is attributed to the local density approximation.

In Fig. 8 we plot the resulting depletion force calculated using our model for different plate separations at $\eta_s^r = 0.3$. For large plate separation, when the density of small particles is uniform or close to uniform, the resulting depletion force compares very well with the simulation results regardless of the density of small particles. This suggests a good performance of the Derjaguin approximation. The depletion force at other plate separations, where the small-particle density is not uniform, develops the same trends as the depletion force of the simulated system, but with a degree of exaggeration. In the real system, therefore, the effect of the nonuniform distribution of the small particles is alleviated. Götzelmann and Dietrich [23] observed that in the slit geometry the layers parallel to the xy plane exhibit stronger correlations at lower density than those at higher density. This happens be-

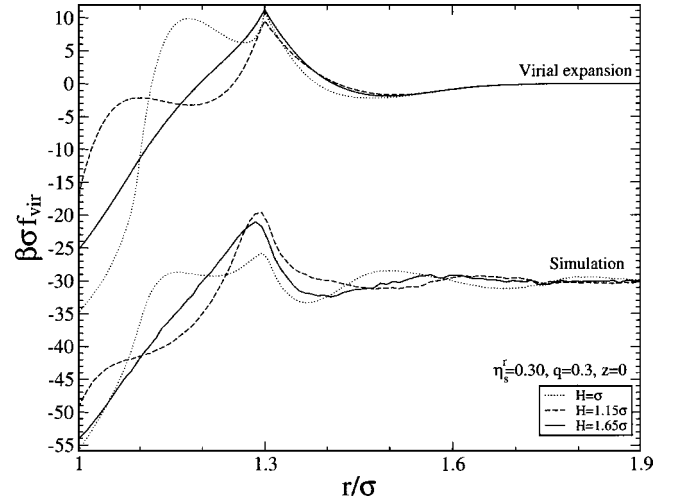


FIG. 8. The depletion force calculated using our model described in Sec. V compared to the exact depletion force calculated from the simulation for different plate separations. The depletion force for the simulation result has been shifted down for presentation purposes.

cause when a low-density region is embedded in a high-density region, it gains some order, otherwise absent in a uniform system. On the other hand, a high-density region surrounded by a low-density region loses some of its order. In this context one may loosely speak of a “conservation of order” being responsible for resisting deviations from a uniform structure. The calculations performed at $\eta_s^r = 0.19$ and $\eta_s^r = 0.25$ indicate that the discrepancy between the virial expansion and the simulation results decreases with decreasing density.

The qualitative agreement between the simulation and the virial expression results for the depletion force permits us to determine the connection between the small-particle density distribution and the depletion force between two large spheres. In Fig. 9 we show the small-particle density profiles along the z axis generated from simulations of the small particles in the slit geometry when no large particles are present. For the largest plate separation, the two outermost peaks are too far from the center of the cell to influence the depletion force between two large spheres located in the central plane. The effects of the secondary peaks are almost invisible. For plate separation $H = \sigma$, the depletion force is enhanced and shifted to smaller particle separation compared to that for the homogeneous case. The shift and enlargement is caused by the outermost peaks whose influence becomes important at smaller particle separation. The shift of the repulsive barrier to lower particle separation produces the reduction of the attractive range of the depletion force. For intermediate plate separation the repulsive barrier and the attractive part of the depletion force are reduced. This indicates that the outermost peaks are already beyond the range where they can influence the depletion interaction between two large spheres. The reduction effect comes from the valleys following the outermost peaks. We conclude that for the density of small particles covered in this work, the effects of confinement on the depletion interaction between two large spheres comes from the outermost region where the density

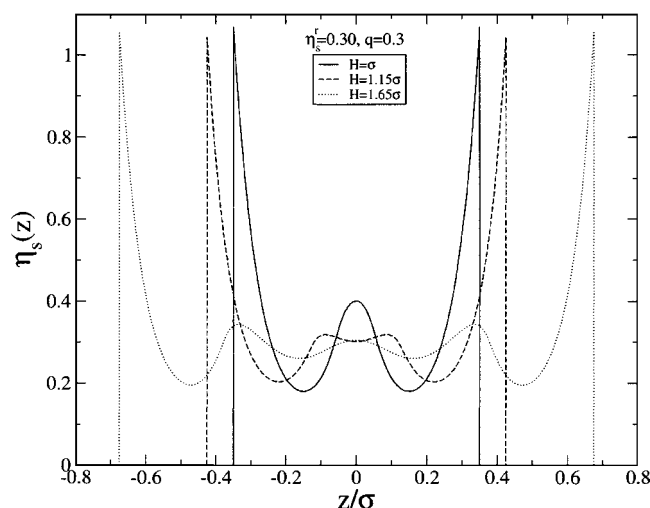


FIG. 9. The small-particle density profiles along the z axis generated from simulations of the small particles in the slit geometry when no large particles are present. $\eta_s(z) = \pi\sigma^3\rho_s(z)/6$.

distribution is mostly distorted. For size ratios less than $q = 0.3$ and the same packing fraction η_s^* , the influence of the confining walls on the depletion interaction is expected to be smaller since the outermost peaks are more narrow and farther removed from the central plane.

VI. CONCLUSION

We have studied the depletion interaction and how this interaction changes with changing the degree of confinement in a Q2D binary hard-sphere mixture with size ratio $q = 0.3$. By going to large plate separation we were able to compare the depletion interaction of the confined system with that for the homogeneous 3D system. Our study focuses on how the heterogeneity of the small-particle distribution affects the depletion interaction between two large spheres in a Q2D slit geometry. Our findings show that the confining walls do not have a very strong overall effect on the depletion interaction.

Not surprisingly, the largest changes in the depletion potential occur when $H = \sigma$, when the confinement is greatest. At this plate separation, both the range and repulsive barrier of the depletion potential are reduced. The range of the wall influence on the depletion interaction is equivalent to the diameter of a small sphere. Another important feature of our results is that the confinement does not produce a monotonically changing influence on the depletion interaction with increasing plate separation, but instead produces a modulating contribution. Both the depletion potential range and the repulsive barrier oscillate as the plate separation increases.

We have also studied the depletion interaction by comparing the simulation results with an idealized model that treats the density of small particles, into which two large particles are immersed, locally without reference to the neighboring region. For large plate separation when the density distribution of small particles is nearly uniform, the resulting depletion force compares very well with that of the simulated system. For smaller plate separation the depletion force calculated from the model develops the same features as that of the simulated system, indicating that the changes in the depletion force are connected with the density distribution of small particles. However, the model gives an exaggerated account of the contributions due to the spatial variation of the small-particle density. This indicates that in a real system there exists a mechanism which counters the effects of the spatial variations of the small-particle density. By investigating the connection between the small-particle density profile and the resulting depletion force, we determined that for η_s^* values covered in this paper it is the outermost peaks together with the adjacent valleys that affect the depletion interaction in any significant way [24].

ACKNOWLEDGMENTS

This research was supported by a grant from the National Science Foundation (No. CHE-9977841). We have also benefited from the support of the National Science Foundation funded MRSEC Laboratory at the University of Chicago.

-
- [1] S. Asakura and F. Oosawa, *J. Chem. Phys.* **22**, 1255 (1954).
 - [2] M. Dijkstra, R. van Roij, and R. Evans, *Phys. Rev. E* **59**, 5744 (1999).
 - [3] T. Biben, P. Bladon, and D. Frenkel, *J. Phys.: Condens. Matter* **8**, 10799 (1996).
 - [4] S. Melchionna and J. P. Hansen, *Phys. Chem. Chem. Phys.* **2**, 3465 (2000).
 - [5] D. Gouling and S. Melchionna, *Phys. Rev. E* **64**, 011403 (2001).
 - [6] R. Castañeda-Priego, A. Rodríguez-López, and J. M. Méndez-Alcaraz, *J. Phys.: Condens. Matter* **15**, S3393 (2003).
 - [7] W. G. McMillan and J. E. Mayer, *J. Chem. Phys.* **13**, 276 (1945).
 - [8] J. R. Henderson, *Mol. Phys.* **50**, 741 (1983).
 - [9] R. Roth, R. Evans, and S. Dietrich, *Phys. Rev. E* **62**, 5360 (2000).
 - [10] B. Götzelmann, R. Evans, and S. Dietrich, *Phys. Rev. E* **57**, 6785 (1998).
 - [11] L. Reatto, D. Levesque, and J. J. Weis, *Phys. Rev. A* **33**, 3451 (1986).
 - [12] N. G. Almaraz and E. Lomba, *Phys. Rev. E* **68**, 011202 (2003).
 - [13] J. A. Barker, D. Henderson, and W. R. Smith, *Mol. Phys.* **17**, 1683 (1969).
 - [14] R. Evans, *Mol. Simul.* **4**, 409 (1990).
 - [15] M. A. van der Hoef and P. A. Madden, *J. Chem. Phys.* **111**, 1520 (1999).
 - [16] A. A. Louis, *J. Phys.: Condens. Matter* **14**, 9187 (2002).
 - [17] D. Frydel and S. A. Rice, *Phys. Rev. E* **68**, 061405 (2003).
 - [18] R. L. Henderson, *Phys. Lett.* **49**, 197 (1974).

- [19] Y. Mao, M. E. Cates, and H. N. W. Lekkerkerker, *Physica A* **222**, 10 (1995).
- [20] J. P. Hansen and I. R. McDonald, *Theory of Simple Liquids* (Academic Press, London, 1986).
- [21] J. Lyklema, *Fundamentals of Interface and Colloid Science* (Academic, London, 1991).
- [22] P. Attard, *J. Chem. Phys.* **91**, 3083 (1989).
- [23] B. Götzelmann and S. Dietrich, *Phys. Rev. E* **55**, 2993 (1997).
- [24] D. Frydel and S. A. Rice (unpublished).